Langmuir

Article

pubs.acs.org/Langmuir

Quantifying Protein Adsorption and Function at Nanostructured Materials: Enzymatic Activity of Glucose Oxidase at GLAD Structured Electrodes

Uffe B. Jensen, Elena E. Ferapontova, and Duncan S. Sutherland*

Interdisciplinary Nanoscience Center (iNANO), Aarhus University, DK-8000 Aarhus, Denmark

Supporting Information

ABSTRACT: Nanostructured materials strongly modulate the behavior of adsorbed proteins; however, the characterization of such interactions is challenging. Here we present a novel method combining protein adsorption studies at nanostructured quartz crystal microbalance sensor surfaces (QCM-D) with optical (surface plasmon resonance SPR) and electrochemical methods (cyclic voltammetry CV) allowing quantification of both bound protein amount and activity. The redox enzyme glucose oxidase is studied as a model system to explore alterations in protein functional behavior caused by adsorption onto flat and nanostructured surfaces. This enzyme and such materials interactions are relevant for biosensor applications. Novel nanostructured gold electrode surfaces with controlled curvature were fabricated using colloidal lithography and glancing angle deposition (GLAD). The adsorption of enzyme to nanostructured interfaces was found to be significantly larger compared to flat interfaces even after normalization for the increased surface area, and no substantial desorption was observed within 24 h. A decreased enzymatic activity was observed over the same period of time, which indicates a slow conformational change of the adsorbed enzyme induced by the materials interface. Additionally, we make use of inherent localized surface plasmon resonances in these nanostructured materials to directly quantify the protein binding. We hereby demonstrate a QCM-D-based methodology to quantify protein binding at complex nanostructured materials. Our approach allows label free quantification of protein binding at nanostructured interfaces.

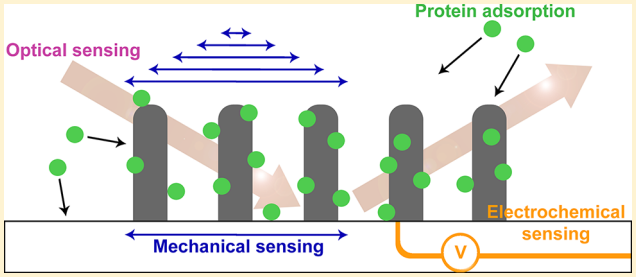

INTRODUCTION

Adsorbed layers of protein mediate the functional properties of materials in many scientific and technological areas including biosensing, tissue engineering, drug delivery devices, and toxicological effects of nanoparticles.[1] The adsorption, desorption, and conformational changes of proteins interacting with surfaces are important processes for understanding the influence on the adsorbed layers. When materials have structures on the nanometer scale, the protein function can be altered.[2−5] Surface-immobilized redox enzymes can be used in electrochemical biosensors, in which the rate of a bioelectrocatalytic reaction carried out by the enzyme is measured.[6,7] There are numerous examples in the literature of electrochemical enzyme-based biosensors or biofuel cells, which often show improved properties owing to immobilization for instance on carbon nanotubes (CNT),[8] carbon nanoparticles,[9] gold nanoparticles,[10] or conducting polymers.[11] Both the total loading of enzyme and also the activity, stability, and electron transfer properties may be altered at the nanostructured surfaces compared to those at a nonstructured flat surface through both strong[2] and weak interactions.[12] This is especially the case when the curvature of a nanostructured surface is comparable to the size of an enzyme.

A key parameter for characterizing such systems is the amount of protein present at an interface. A number of approaches based on optical readout have been successfully and widely applied to interfaces with flat geometry, e.g., surface plasmon resonance[13] (SPR), ellipsometry,[14] and optical waveguide lightmode spectroscopy[15] (OWLS). Protein quantification by such approaches is complicated at structured interfaces that intrinsically scatter light. While probe-based approaches such as radio labeling can be applied, they provide their own limitations; e.g., radio labeling techniques are not surface sensitive and are not suited for *in situ* kinetic measurements.[16] Using electrochemistry only the electrochemically active enzymes can be addressed, and the situation is further complicated by the fact that the rate constants of the bioelectrocatalytic reaction might change. Therefore, optical and electrochemical methods are often poor choices for measuring the total amount of protein on a structured surface. Atomic force microscopy has proven applicable to the use on moderately rough surfaces where individual proteins can be resolved, e.g., rigid proteins on supported lipid bilayers.[17] Recent work with the quartz crystal microbalance have shown it can be applied for dense films both nanopatterned[18] and moderately rough surfaces (up to 6 nm rms).[19]

Received: April 30, 2012
Revised: June 29, 2012
Published: July 2, 2012

In this study the enzyme glucose oxidase (GOx) was immobilized onto flat as well as on nanostructured gold electrode surfaces as a model system. GOx was chosen as a model enzyme because it is relatively well-studied and it is widely applied in commercial glucose biosensors because of its advantageous properties, e.g., high selectivity for glucose oxidation.[20] GOx is relatively stable to inactivation,[21] and it could therefore be expected to retain a significant amount of activity at a metal−aqueous solution interface. There are already commercial glucose biosensors based on GOx in use for diabetes treatment. Such sensors could be applied to give better therapy by developing implantable glucose sensors, but before these can be successful, issues concerning enzyme stability and biocompatibility of such devices must be addressed.[22] Chemical cross-linking of GOx, including binding to Os−complex redox polymers, or entrapment in micelles have previously been used to enhance enzyme stability,[21,23] but it is still clear that the interface at which immobilization takes place is an important factor.

A quartz crystal microbalance with dissipation monitoring (QCM-D) was used along with conventional optical and electrochemical methods, which enabled the investigation of nanostructured surfaces. A novel approach to interpreting the QCM-D signal was applied, since QCM-D is not routinely applied to highly rough surfaces. The experiments demonstrate that the nanostructured material critically affected both the adsorption kinetics and catalytic rate constants of glucose oxidase as compared to flat surfaces. The surfaces used for immobilization were produced via colloidal lithography[24] and glancing angle deposition.[25,26] This nanofabrication method allows for control over the curvature of the surface.

Surface immobilization of enzymes or proteins can lead to alterations of their conformation where the surface energy of the material plays a critical role. For instance, at a hydrophobic material, conformation alteration revealing buried hydrophobic domains can provide a driving force for adsorption. Such conformational changes may affect the activity and stability of adsorbed enzyme.[27] The extent of surface adsorption and conformational change of a protein depends on surface chemistry, topography, and properties of the protein itself.[28] It is expected that structures on the micrometer scale such as carbon cloth[29] would primarily increase the amount of adsorbed protein as the surface roughness is large, while nanometer-sized structures could have additional effects, since they are similar in size to an individual protein.

RESULTS AND DISCUSSION

Fabrication of nanostructured surfaces was performed combining colloidal lithography with glancing angle deposition (GLAD). This methodology allows for structuring of large surface areas, while retaining a relatively large control of the structures. Nanostructured gold electrodes were prepared on silicon wafers or directly on QCM-D sensor crystals. Gold nanoparticles were dispersed on a gold surface producing a short-range ordered array of nanoparticles, which was used as a template for GLAD. The resulting nanostructure (Figure 1a) can be approximately described as composed of cylindrical pillars with a hemispherical top. Estimation from SEM images gives a diameter of 49.3 ± 6.5 nm and a height of 65.0 ± 5.9 nm, and thus the radius of curvature is of the same order of magnitude as the size of many proteins. The electrochemically accessible surface area was determined from the gold surface oxide reduction peaks in cyclic voltammetry (CV) recorded in

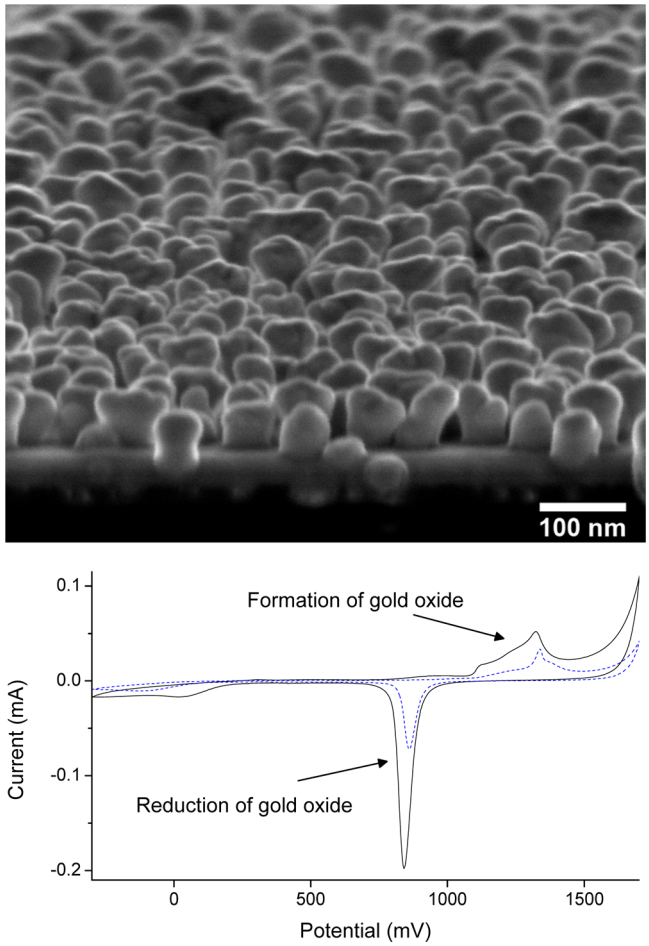

Figure 1. (top) Nanosize pillars produced with GLAD. SEM image with an 80° tilt angle. (bottom) Representative CVs of flat (dotted line) and GLAD (solid line) gold electrodes, recorded in 0.1 M H_2SO_4, potential scan rate 40 mV/s. Reduction peaks corresponds to the electroreduction of gold surface oxides formed during the oxidation cycle.

0.1 M H_2SO_4[30] (Figure 1b) to be 2.91 ± 0.09 times that of a flat gold surface. This ratio, often called the roughness factor, can also be estimated based on the SEM images yielding a value of 3.1 ± 0.3, which is consistent with the electrochemically measured value. We did not observe any changes to the nanostructured surfaces after the electrochemical experiments when imaged by SEM.

Protein adsorption measurements with the QCM-D were performed with 0.20 mg/mL GOx. Experiments at higher and lower GOx concentrations showed no significant difference for concentrations above 0.10 mg/mL. The effect of ionic strength was studied using two different buffers: 5 and 20 mM sodium phosphate at pH 7.0. Representative QCM-D graphs are shown in Figure 2. At time t = 0 the buffer in the chamber was replaced with GOx solution, and after ca. 20 min pure buffer was again introduced to allow loosely bound protein to desorb. Largely irreversible protein adsorption to both surfaces is observed as seen from the reduction in frequency during exposure to protein solution. There was a clear difference between flat and nanostructured surfaces in the magnitude of the frequency shift, which was several times larger for the nanostructured surfaces, indicating more protein binding. Furthermore, almost no desorption was observed for nanostructured

dx.doi.org/10.1021/la3017672 | Langmuir 2012, 28, 11106−11114

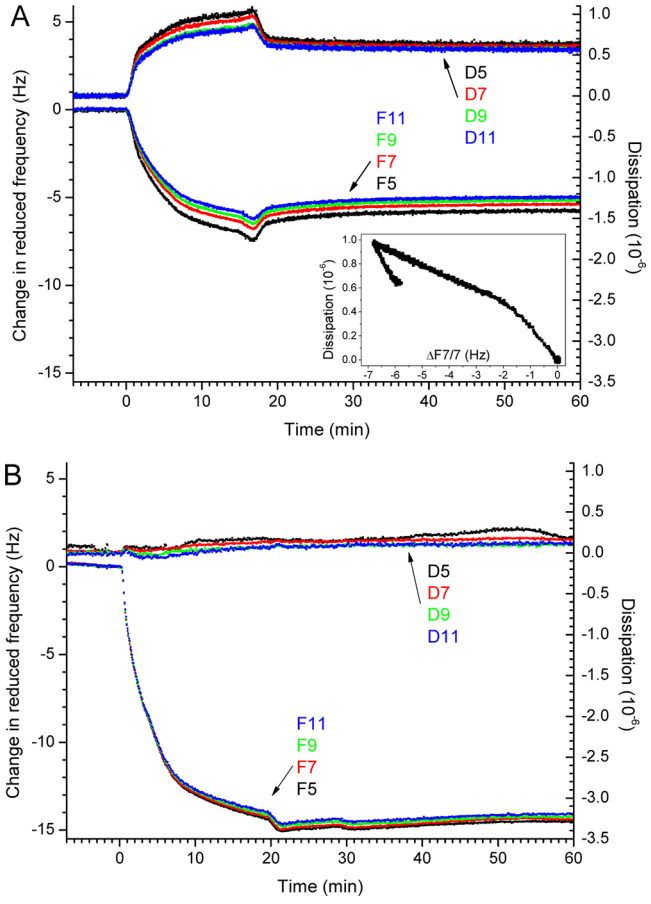

Figure 2. Representative QCM-D experimental data, where both frequency, *F*, and dissipation, *D*, are shown; numbers stand for overtones. At time zero GOx when injection begins adsorption is observed for flat (A) and GLAD (B) gold surface. After completed injection at ca. 20 min a small amount of desorption takes place. Both the reduced frequency and dissipation changes are shown for both flat and GLAD surfaces for the 5th to 11th overtone. (A, inset) Dissipation plotted versus reduced frequency for the 7th overtone.

surfaces, while the total mass adsorbed onto flat surfaces was reduced by ∼21% after 1 h. Thereafter, no significant desorption was observed. Note that QCM-D is not suitable for protein structure determination. Although some structural changes could potentially affect the change in dissipation, ΔD, the change in frequency, ΔF, mainly denotes changes in the surface coupled mass.

Plots of ΔD vs ΔF can reveal details of the adsorption process by removing time explicitly from the data. For flat surfaces the ΔD vs ΔF plot shows two distinct regions with a linear relationship between frequency and dissipation (Figure 2a, inset), which suggests two types of adsorption takes place with a higher and a lower dissipation per frequency. The protein that desorbed showed a higher dissipation per frequency change. During protein adsorption to nanostructured surfaces almost no dissipation changes were observed despite substantial changes in frequency.

Quantification of the adsorbed mass can be performed with the Sauerbrey equation if the adsorbed layer is rigid.[31,32] The results presented in Table 1 show a larger protein mass on the nanostructured GLAD surfaces than on flat surfaces according to the Sauerbrey equation. Since the protein is nonrigid and since the nanostructure is expected to affect QCM-D measurements, it is not expected that the Sauerbrey equation is accurate, but it is still qualitatively useful for comparison.

For flat surfaces with homogeneous nonrigid layers that dissipate energy the Voigt model can be used, in which the reduced coupling between the crystal and the bulk solution is also taken into account. This model includes parameters for the viscoelastic properties of the adsorbed layer as well as the bulk solution. Frequency and dissipation changes for different overtones are predicted by the model.[33] Modeling was performed for the flat surface QCM-D data (Table 1). In the modeling the thickness and density of such a layer are not independent variables, and while the Voigt mass is reasonably well-defined, to establish the films density or thickness explicitly requires an additional technique. Ellipsometry,[34] atomic force microscopy[18] (AFM), and surface plasmon resonance[35] (SPR) are methods that have been used to provide additional information.

In this study SPR was used to independently quantify the amount of protein on the flat surfaces. In SPR a change in refractive index is measured, i.e., relative to the refractive index of buffer. Therefore, only the dry mass of protein is measured in contrast to the QCM-D measurements, where protein-bound water contributes to the signal.[13,36] Because of light scattering, SPR cannot be performed on structured surfaces. The SPR instrument was calibrated using solutions of glucose with known refractive indices. In the thin film limit the SPR signal is proportional to the mass of adsorbed material, but a more accurate surface mass density can be determined if the film thickness, *d*, is known using the equation[35]

$$\Gamma_{SPR} = d\frac{dc}{dn}\kappa\frac{\Delta\Theta}{1-\exp\left(-\frac{2d}{l_{decay}}\right)}$$

where dc/dn is the relation between changes in refractive index and concentration, κ is a sensitivity coefficient, $\Delta\Theta$ is the change in SPR angle, and l_{decay} is the decay length for the evanescent wave.

Now an iterative approach[18] was used, where the thickness of the protein layer was obtained from QCM-D modeling. This thickness was then used to obtain a more accurate value of the mass determined by SPR, from which the layer density can be

Table 1. Summary of Adsorbed Protein Mass Results Based on QCM-D, SPR, and LSPR Methods[a]

	flat gold surface			nanostructured gold surface		
phosphate buffer concn (mM)	$\Gamma_{Sauerbrey}$, ng/cm^2	Γ_{Voigt},[b] ng/cm^2	Γ_{SPR},[c] ng/cm^2	$\Gamma_{Sauerbrey}$, ng/cm^2	$\Gamma_{corrected}$,[b] ng/cm^2	Γ_{LSPR},[c] ng/cm^2
5	68.6 ± 30.1	95.1 ± 37.1	32.3 ± 6.4	185 ± 34	501 ± 92	104 ± 27
20	118 ± 15	160 ± 25	50.3 ± 5.8	234 ± 33	660 ± 93	165 ± 43

[a]Γ is the surface density calculated from respectively the Sauerbrey equation, the Voigt model, SPR determined value, corrected for the effect of the nanostructured using the coupling efficiency, and LSPR value. [b]Protein wet mass, including the mass of protein bound water. [c]Protein dry mass, not including protein bound water.

dx.doi.org/10.1021/la3017672 | *Langmuir* 2012, 28, 11106−11114

calculated. The new density was then used to improve the QCM-D model and so on.[18] Convergence was typically reached after 2−3 iterations (Table 1). Here the density of the protein layer was found to be 1087 kg/m^3, which corresponds to ca. 67% of the Voigt mass stemming from water.

The dry mass surface density can be converted into surface concentrations using the molecular mass of GOx of 160 kDa:[37] σ = 0.202 and 0.314 pmol/cm^2 for respectively 5 and 20 mM phosphate buffer, corresponding to footprint sizes of 823 and 528 nm^2, which are substantially larger than the largest cross-sectional area of GOx of 46.2 nm^2 predicted from protein structure.[38] Szucs and co-workers have found surface coverages up to 1.5 pmol/cm^2 as determined by ellipsometry; however, this was done using different protein concentrations and buffer conditions.[39]

Comparing the two ionic strengths, significantly more adsorption was observed in 20 mM than in 5 mM buffer (t test, p = 0.05, n = 4). This indicates that the electrostatic forces at the solid−liquid interface are important. GOx, with a pI of 4.2,[20] is negatively charged at pH 7, and an increased screening at 20 mM could therefore explain the higher surface coverage, since the protein−protein repulsion is lower (Table 1).

For rough surfaces it is more difficult to directly relate the QCM-D signal to the amount of mass adsorbed.[19] The most important issue is that water is expelled from the nanostructure as protein is adsorbed. Therefore, the entire hydrated mass of the protein is presumably not detected as it would be on a flat surface, rather only the change owing to the density difference of water and protein. An additional important issue is that water coupled to the protein may be more strongly coupled to the crystal oscillations than bulk water. If the water within the nanostructure was strongly coupled to the crystal, it could be treated as a rigid layer, of which the density changed upon protein adsorption. Given that the binding of GOx to flat gold led to a significant increase in the dissipation, the lack of significant change in dissipation during protein adsorption at the nanostructured interface strongly supports the idea that the water in the nanostructures is already strongly coupled to the crystal oscillations. In order to be quantitative, it is necessary to determine how strongly the water is coupled to the oscillations of the crystal; therefore, measurements in air and in buffer were performed for both flat and nanostructured surfaces (data shown in Table S1) in order to evaluate how strongly the water close to the nanostructures is coupled to the oscillations of the crystal. According to the Kanazawa equation,[32] the difference between measurements in air and in buffer should be $\Delta f_N = (-{f_N}^{3/2}/N)(\rho_l\eta_l/\pi\rho_q\mu_0)^{1/2}$ and $\Delta D_N = 2({f_N}^{1/2}/N)(\rho_l\eta_l/\pi\rho_q\mu_0)^{1/2}$, where f_N is the fundamental frequency for the Nth overtone, ρ_l and η_l are density and viscosity of the liquid, and ρ_q and μ_q are density and shear modulus of the quartz crystal. These equations gave a good description of the data from flat surfaces, but for the nanostructured surfaces an additional effect was seen in the relation. The difference between the reduced frequency changes for nanostructured and flat surfaces, $\Delta f_N^{nano}/N - \Delta f_N^{flat}/N$, was almost constant although the values decreased slightly with N (see Table S1). The additional frequency shift stems from water within the nanostructure being strongly coupled to the QCM crystal in addition to water outside the nanostructure. Applying the Sauerbrey equation, the difference in frequency shift when switching from air to fluid and subtracting the flat from the structured surface corresponds to 2840 ± 581 and 2906 ± 661 ng/cm^2 for the two buffers. These values represent effective surface mass densities, which contain information about how strongly the solution is coupled to the crystal surface. The relatively large errors are likely due to differences in humidity from day to day or simply variation between samples of nanostructured surfaces.

We make use of detail of the nanostructured material to independently determine the amount of solution within the nanostructured layer. Using the average pillar height of the nanostructures, the size and density of AuNPs, and the volume of metal deposited during the GLAD process, we find that the pore volume of the nanostructure contains Γ_{real}^{water} = 4147 ng/cm^2 of solution. We now define a coupling efficiency ϕ representing the extent to which the fluid within the nanostructure is coupled to the crystal oscillation as the ratio of the effective surface density determined by QCM-D and the real surface density of solution within the nanostructure. For the nanostructures used in this study the coupling efficiencies are $\phi_{5\ mM}$ = 0.685 and $\phi_{20\ mM}$ = 0.701. The surface mass density of protein at the nanostructure can now be determined from the QCM-D frequency shift assuming that partially coupled water in the nanostructured surface is replaced by protein rigidly coupled to the oscillations and using a correction factor equal to the ratio of the protein density and an effective protein density that depends on ϕ:

$$\Gamma_{corrected} = \Gamma_{Sauerbrey}\frac{\rho_{protein}}{\rho_{protein} - \phi\rho_{water}} \qquad \phi = \frac{\Gamma_{Sauerbrey}^{water}}{\Gamma_{real}^{water}}$$

The densities used here were ρ_{water} = 1000 kg/m^3 and $\rho_{protein}$ = 1087 kg/m^3. In this equation the density of hydrated protein should be used because protein-bound water couples much more strongly with the quartz crystal oscillations than bulk water. The protein density was assumed to be the same as for flat surfaces, which was determined by SPR combined with QCM-D using viscoelastic modeling. The above equation is based on the assumption that all water within the nanostructure that is replaced by protein is originally coupled with the same efficiency, but it is likely that the coupling efficiency depends on the adsorption site. The experimentally determined coupling efficiency represents an average value for all the sites and is appropriate for a homogeneously distributed protein deposition. The fact that very little change in dissipation is observed for the structured surfaces implies that modeling is not required. This is presumably because water above the nanostructure is unaffected by protein adsorption inside the structure; thus, the corrected Sauerbrey equation may be applied.

The resulting corrected QCM-D values of the protein surface density are significantly larger than those found for flat surfaces. In fact, 4−5 times more protein was found to adsorb to the nanostructured surfaces compared to flat surfaces, which is significantly more than the increase in surface area of about 2.9 times. Increased amounts of protein binding per surface area have previously been reported for rough surfaces,[40] but the physical basis for this observation has not yet been established.

In order to verify the applicability of the above-mentioned method, where QCM-D is used on structured surfaces, another independent measure of the amount of protein was used. Fortuitously, this nanostructured material has useful plasmonic properties (Figure 3a), where a reduced reflection is observed at certain wavelengths. This is interpreted as absorption of light by excitation of localized surface plasmon resonance (LSPR) in the nanostructure. The spectral position of such a LSPR depends on the refractive index of the surroundings. Using thiols of

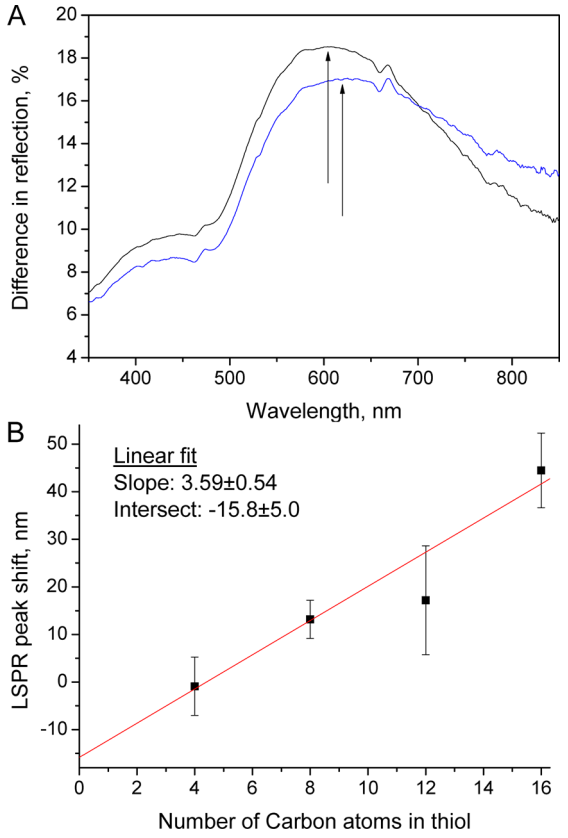

Figure 3. (A) Representative UV−vis reflection difference spectra of GLAD nanostructure before (black line) and after (blue line) adsorption of GOx, with subtraction of background spectrum of 30 nm gold film. Arrows mark the position of the peak, which shifts to larger wavelengths upon GOx adsorption. (B) LSPR peak shift after adsorption of different length alkanethiol molecules. A linear fit was performed (red line).

different lengths, a calibration curve was constructed and a linear relationship was found between the shift in wavelength of the LSPR and the number of carbon atoms in the alkanethiol molecule (Figure 3b).

The adsorption of GOx resulted in a peak shift of 6.18 nm for the low ionic strength and 9.81 nm for the higher ionic strength. By using the alkanethiol-based calibration curve and correcting for the difference in refractive index, the peak shifts are found to correspond to surface mass densities of 35.8 and 56.8 ng/cm^2 for the 5 and 20 mM buffers, respectively. These LSPR-derived values for the amount of protein per area are larger than the ones found for flat surfaces (SPR). Notice that this is the density per real surface area; in order to make it comparable to the other mass densities, per projected area, the value was multiplied by the roughness factor of the nanostructures (see Table 1). It is difficult to draw conclusions about the accuracy of the methodology; however, the LSPR results are consistent with the corrected QCM-D results for nanostructured materials and support the approach used to quantify the protein adsorption at the nanostructured materials using QCM-D.

Comparing Γ_{SPR} to Γ_{Voigt} and Γ_{LSPR} to $\Gamma_{corrected}$, we obtain information about the amount of water coupled to the protein, which is measured in the QCM-D. This reveals that more water is present at the proteins on the nanostructured surface. This might be caused by a lesser degree of unfolding at the nanostructure, but it cannot be ruled out that QCM-D is more sensitive to protein bound water at nanostructured interfaces.

The values from corrected QCM-D and LSPR indicate increased amounts of protein adsorption on the nanostructured material. Physically, the curvature of a rough or structured surface would allow spherical proteins to be packed closer than on a flat surface. Since the contact points of spheres at a surface are raised from the surface by the sphere radius, in a curved geometry this can lead to an effectively larger surface area for adsorption. Simple geometric calculations show that the effect could only lead to a few percent additional binding on this nanostructure. Furthermore, it should be noticed that negative curvature would have the opposite effect, which is also present at this surface.

Additionally, it is observed that the increase in adsorption with increasing ionic strength is less pronounced on structured surfaces. Assuming that the effect of increasing the ionic strength is to screen the charges of proteins, this would suggest that the nanostructures themselves were able to some extent to screen charges and thus reduce the repulsion between proteins. This suggestion can be rationalized by considering image charges in the metal, which on a curved surface can be positioned between or partly between the proteins. We observe a higher protein binding per surface area at nanostructured surfaces compared to flat. We associate this additional protein binding to alterations in electrostatic protein−protein interactions arising from the curvature of the nanostructured materials. At lower pH than used here GOx is less charged, which is consisted with higher GOx loading;[39] therefore, it is expected that the effect of ionic strength will be less pronounced at lower pH.

The surface amount and catalytic activity of GOx adsorbed onto flat and GLAD surfaces working as electrodes was electrochemically assessed. Bioelectrocatalysis of the oxidation of glucose by GOx can be monitored electrochemically with several approaches.[41] The easiest way is when the direct electron transfer (ET) communication between the electrode surface and the active center of the enzyme can be established.[7] However, the efficient ET generally requires a specific orientation of the enzyme on the electrode surface,[42] which was shown to be difficult to achieve in the case of direct ET reaction between the FAD/FADH$_2$ cofactor of GOx and the electrode.[21] Another approach is to study the mediated ET, which uses a soluble mediator that shuttles electrons between the cofactor of the enzyme and the electrode surface. By this means, not only the electrochemically active (in direct ET reaction) but also total amount of the catalytically active adsorbed enzyme can be detected through the mediated bioelectrocatalysis. This approach is somehow similar to the enzymatic catalysis, with the exception that mediator is electrochemically active and it oxidation state necessary for bioelectrocatalysis is electrochemically regenerated. In the present work the mediator ferrocene methanol (or (hydroxymethyl)ferrocene) was used as a suitable mediator.[43]

Representative cyclic voltammograms of GOx on flat and nanostructured surfaces in the presence of 200 mM glucose are shown in Figure 4. The catalytic currents observed were 8.54 ± 1.64 and 11.3 ± 3.4 μA/cm^2 for flat and nanostructured surfaces, respectively. The relatively large sample to sample deviations are probably caused by differences in surface coverage of the electrodes. The larger current observed at the nanostructured electrode can be explained by a higher loading of enzyme; however the difference is smaller than expected

dx.doi.org/10.1021/la3017672 | Langmuir 2012, 28, 11106−11114

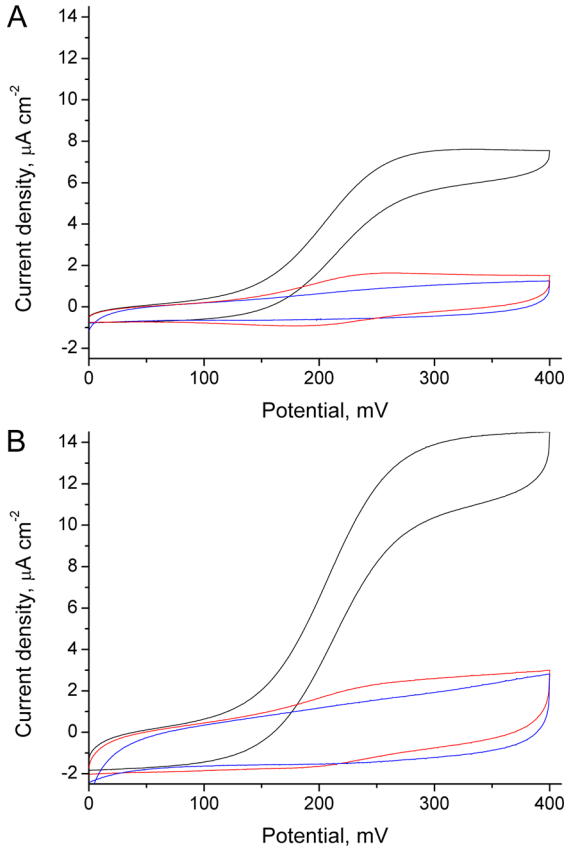

Figure 4. Voltammograms showing bioelectrocatalytic oxidation of glucose at electrodes coated with GOx in 5 mM phosphate buffer, pH 7. (A) GOx immobilized on a flat surface. (B) GOx immobilized on a nanostructured GLAD surface. Blue curves are backgrounds in buffer. Red curves are in presence of 10 μM FcMe as a mediator. Black curves are in the presence of 200 mM glucose and the mediator.

based on the previously determined amounts of enzyme. The Michaelis constant, $K_{M,glucose}$, for GOx depends on the surface of immobilization, and on gold it has been reported to be around 7.5 mM at neutral pH.[44] For the present gold structures we found $K_{M,glucose}$ to be around 20 mM. Since the glucose concentration used in the experiments is considerably larger than $K_{M,glucose}$, the glucose diffusion is not expected to cause a significant limitation to the catalysis; thus, the catalytic currents are approximately proportional to the number of active enzymes on the surface. Therefore, a reduced enzyme activity on nanostructured surfaces must be the reason for the smaller catalytic current per enzyme, since a similar concentration of the substrate was used. Product inhibition is not expected to be large since the surface concentration of GOx is relatively low.[45]

The catalytic rate constant of glucose oxidation can be determined from the catalytic current and the amount of enzyme present on the surface. Assuming that the mediator is present in relatively large amounts, it would not pose any limitation to the bioelectrocatalytic reaction rate; thus, we can use the following equation to calculate k_{cat}:[46]

$$V_{max} = \frac{k_{cat} C_{enzyme}}{1 + \frac{K_{M,glucose}}{C_{glucose}}}$$

This equation can be applied here if $V_{max} = V_{catalytic\ current}$, which is only a good approximation when the glucose concentration is very large and mass transport therefore can be ignored. Therefore, we are likely to underestimate k_{cat} in the following calculation. The total amount of enzyme, C_{enzyme}, is determined using SPR and LSPR values, which results in $k_{cat}^{apparent}$ = 219 ± 60 s^{-1} for flat and $k_{cat}^{apparent}$ = 90.0 ± 29.1 s^{-1} for nanostructured electrode, indicative of a partial deactivation of GOx on nanostructured materials. A possible explanation for this is that the higher loading on nanostructured interfaces leads to stronger protein−protein interactions, which may lead to inactivation.

In order to determine the stability of adsorbed GOx, the bioelectrocatalytic currents of glucose oxidation were measured again after 24 h electrode storage at room temperature. The stability is a very important parameter for biosensors that are meant to function over longer periods of time, e.g., as implantable devices. It could be expected that the nanostructure will affect the stability since the kinetics of denaturation is likely to be affected by the curvature present in a structured surface. Desorption is not expected to play a large role for the stability of GOx, since only small amounts of desorption was observed with QCM-D over 24 h.

The currents after 24 h were found to drop to an average of 44.6 ± 4.2% for flat versus 55.4 ± 6.7% for nanostructured electrodes of the currents measured immediately after adsorption, which is not a statistically significant difference (t test, n = 4, df = 6, p = 0.05). While there appears to be an initial denaturation of GOx on the nanostructured gold surface, the long-term stability is as good as or perhaps better than GOx on flat gold. Further, the capacitive current was found to be smaller after 24 h, which is an indication that the electrode is increasingly blocked by enzymes resulting from such conformational changes as protein unfolding.

Comparing the curvature of this particular nanostructure (radius of curvature ∼25 nm) to the size of GOx (radius 3−4 nm),[38] it could be expected that structures with smaller feature sizes would have an even larger effect on the protein−interface interactions. It is known that some nanomaterials, for example CNTs,[8] have a large effect on enzymes. However, it is often difficult to precisely control properties such as curvature and roughness. When investigating the effect of curvature the chemical nature of the interface should remain constant, which is not the case for CNTs. Therefore, the GLAD nanostructuring approach is well suited for studying the effect of curvature or roughness.

A simple model to describe the observed results is that the nanostructured surface contains sites of different quality for enzyme adsorption, meaning that some sites would promote denaturation while others would stabilize enzymes. If a large proportion of the enzymes are denatured and thus lose catalytic activity within minutes or seconds, this would explain why there is only a 53% larger catalytic current on nanostructured surfaces with 4−5 times more enzymes present. The decrease in current after 24 h was very similar for the two types of electrodes, but it is conceivable that a few particularly good sites on the nanostructured electrodes are able to enhance long-term stability of GOx.

■ CONCLUSION

We have developed an approach to quantify the level of protein adsorbed at nanostructured interfaces. The adsorption of the redox enzyme GOx was studied on flat and nanostructured gold surfaces. QCM-D and SPR were combined in order to quantify the amount of enzyme and level of hydration on flat surfaces. For nanostructured surfaces a novel method was applied, in

dx.doi.org/10.1021/la3017672 | Langmuir 2012, 28, 11106−11114

which the QCM-D data were analyzed by looking at the coupling efficiency of solution to the nanostructure. This was critical because water is expelled from the structure as protein adsorbs, which is not the case in QCM-D on flat surfaces. The additional mass found to adsorb on the nanostructured surfaces was larger than the additional surface area compared to the flat surfaces.

In electrochemical experiments larger currents were found for the nanostructured surfaces, but the apparent catalytic rate constant was lower as compared to flat surfaces. No significant difference in long-term stability was found. The results show a higher loading of enzymes on nanostructured surfaces than on flat, but also an initial partial deactivation of the enzymes, which is probably due to conformational changes at the structured interface. The hypothesis is that the nanostructured interface has two types of sites, able to increase or decrease GOx stability. It is likely that a nanostructure with even smaller features will have a larger impact on the function of enzymes, as the radius of curvature of this nanostructure was several times larger than the radius of GOx.

EXPERIMENTAL SECTION

Materials. All solutions were prepared with deionized Biocell Milli-Q water (18 MΩ·cm, Millipore, Bedford, MA). QCM-D, SPR, LSPR, and electrochemical experiments were performed in sodium phosphate buffer solutions at two different ionic strengths: 5 or 20 mM, pH 7.0. Purified preparations of *Aspergillus niger* glucose oxidase (GOx) have been kindly provided by Novozymes A/S (Denmark). 0.2 mg/mL enzyme solutions were prepared by diluting GOx stock solution in sodium phosphate buffer (5 or 20 mM phosphate).

Nanofabrication. Silicon wafers (Litcon AB, Sweden) were sputter-coated at room temperature (argon pressure 0.2 Pa) with 5 nm titanium and 30 nm gold. Nanostructuring was performed on sputter-coated gold surfaces as well as on gold-coated AT-cut quartz crystals (Q-Sense AB, Gothenburg, Sweden, model QSX 301) using a combination of colloidal lithography and glancing angle deposition (GLAD): The substrate was given a net positive charge at neutral pH by exposure to a solution of 2 wt % polydiallyldimethylammonium chloride (PDDAC) and 20 mM NaCl for 30 s followed by rinsing with MQ water for 60 s and drying with N_2 gas. Then a colloidal suspension of 30 nm gold nanoparticles (BBInternational, United Kingdom) was placed on the substrate overnight, after which the substrate was rinsed with water, dried under N_2 flow, and cleaned with UV-ozone. Subsequently, 3.86×10^{-5} g/cm^2 gold (effectively 20.0 nm film thickness) was deposited by GLAD, which was performed by e-gun stimulated thermal evaporation from an angle 85° relative to the substrate normal. The evaporation was carried out with substrate rotation (6 min^{-1}) at room temperature in vacuum $<10^{-8}$ mbar with a distance between substrate and evaporation source of 25 cm. Characterization was performed on a Magellan 400 (FEI Co.) scanning electron microscope (SEM). Substrates stored more than a day were cleaned with UV-ozone before use.

Quartz Crystal Microbalance with Dissipation Monitoring. QCM-D was performed on a QCM E4 instrument (Q-sense AB, Sweden) with 4.95 MHz AT-cut gold-coated quartz crystals (type QSX 301). The crystals were used as received or after the nanofabrication procedure. Crystals were cleaned with a 1 wt % SDS solution, ethanol, and UV-ozone treatment. Buffers were filtered and degassed using ultrasound in order to avoid gas bubble formation. Flow rate was 100 μL/min, and temperature was kept at 25.00 ± 0.02 °C. When a stable baseline had been observed for at least 30 min, the adsorption process was initiated by exchanging buffer with enzyme solution. After 20 min the flow was changed back to buffer for at least 1 h.

Surface Plasmon Resonance. SPR experiments were carried out on a Biacore X instrument (Biacore AB, Sweden). SPR sensor chips (SIA-Au) were purchased from GE Healthcare (United Kingdom) and cleaned in a 3:1 mixture of NH_4NO_3 and 30 wt % H_2O_2 (Sigma-Aldrich) heated to ca. 70 °C, then UV-ozone treated, and rinsed in water. Buffers were used as in QCM-D experiments. With a flow rate of 20 μL/min, a volume of 80 μL enzyme solution was injected into the flow cell for the adsorption process, followed by buffer flow for at least 20 min. In parallel with the experiment a control channel without enzyme flow was used to correct for signal drift.

Localized Surface Plasmon Resonance. UV−vis spectra were measured with a Shimadzu UV-3600 UV−vis−NIR spectrophotometer with an integrating sphere. Reflectance was measured with the beam 8° to the normal. Reflectance spectra were recorded before and after thiolation of the GLAD structures as well as before and after adsorption of GOx. Butane-1-thiol, octane-1-thiol, dodecane-1-thiol, and hexadecane-1-thiol were used as received from Sigma-Aldrich. In order to determine the peak positions, a fourth degree polynomial was fitted to the region around the peak. In some cases irrelevant absorption peaks at 555−580 and 655−675 nm were masked from the fitting procedure. The calculation of surface density was done by correcting for the refractive index (1.50 for thiols and 1.41 for protein relative to 1.00 for air) and then multiplying with the slope of the calibration curve and the density of dry protein (1.42 g/cm^3).

Electrochemistry. Cyclic voltammetry (CV) was done in a three-electrode cell using the potentiostat AUTOLAB PGSTAT 30 (Eco Chemie B. V., Utrecht, Netherlands) equipped with the GPES 4.9.006 software. An Ag/AgCl (4 M KCl) electrode was the reference, and a platinum flag was the auxiliary electrode. The flat or GLAD gold plates fitted in homemade Teflon holders were the working electrodes. The surface of the working electrode area exhibited to the working solution was restricted by a 3.5 mm diameter rubber O-ring. The working solution was deaerated with nitrogen for at least 30 min prior to data acquisition and was blanketed under N_2 during the entire experimental period. GOx was adsorbed onto gold electrodes by placing 10 μL of 0.2 mg/mL GOx onto the electrode surface for 20 min. The experiments were carried out at room temperature 21 ± 1 °C. For stability measurements samples were stored in phosphate buffer, pH 7, at room temperature for 24 h.

ASSOCIATED CONTENT

Supporting Information

Surface plasmon resonance data plotted as a function of time; quartz crystal microbalance data; and cyclic voltammograms showing the enzyme activity after 24 h. This material is available free of charge via the Internet at http://pubs.acs.org.

AUTHOR INFORMATION

Corresponding Author

*E-mail: duncan@inano.au.dk.

Notes

The authors declare no competing financial interest.

ACKNOWLEDGMENTS

The authors thank Novozymes A/S for the preparation of *Aspergillus niger* glucose oxidase. The authors also thank Jacques Chevallier and Folmer Lyckegaard for technical assistance regarding thin film depositions. The authors are grateful to the EU for financial support in the framework of the project "3D-Nanobiodevice" (NMP4-SL-2009-229255).

REFERENCES

(1) Kasemo, B. Biological surface science. *Curr. Opin. Solid State Mater. Sci.* **1998**, *3* (5), 451−459.

(2) Vertegel, A. A.; Siegel, R. W.; Dordick, J. S. Silica nanoparticle size influences the structure and enzymatic activity of adsorbed lysozyme. *Langmuir* **2004**, *20* (16), 6800−6807.

(3) Sutherland, D. S.; Broberg, M.; Nygren, H.; Kasemo, B. Influence of nanoscale surface topography and chemistry on the functional

behaviour of an adsorbed model macromolecule. *Macromol. Biosci.* **2001**, *1* (6), 270−273.
(4) Zhu, R.-R.; Wang, W.-R.; Sun, X.-Y.; Liu, H.; Wang, S.-L. Enzyme activity inhibition and secondary structure disruption of nano-TiO2 on pepsin. *Toxicol. In Vitro* **2010**, *24* (6), 1639−1647.
(5) Sabirianov, R. F.; Rubinstein, A.; Namavar, F. Enhanced initial protein adsorption on engineered nanostructured cubic zirconia. *Phys. Chem. Chem. Phys.* **2011**, *13* (14), 6597−6609.
(6) Ghindilis, A. L.; Atanasov, P.; Wilkins, E. Enzyme-catalyzed direct electron transfer: Fundamentals and analytical applications. *Electroanalysis* **1997**, *9* (9), 661−674.
(7) Ferapontova, E. E. Unmediated enzyme electrodes. In *Encyclopedia of Sensors*; Grimes, C. A., Dickey, E. C., Eds.; American Scientific Publishers: Valencia, CA: 2006; Vol. *10*, pp 391−422.
(8) Gooding, J. J. Nanostructuring electrodes with carbon nanotubes: A review on electrochemistry and applications for sensing. *Electrochim. Acta* **2005**, *50* (15), 3049−3060.
(9) Jensen, U. B.; Vagin, M.; Koroleva, O.; Sutherland, D. S.; Besenbacher, F.; Ferapontova, E. E. Activation of laccase bioelectrocatalysis of O2 reduction to H2O by carbon nanoparticles. *J. Electroanal. Chem.* **2012**, *667*, 11−18.
(10) Pingarron, J. M.; Yanez-Sedeno, P.; Gonzalez-Cortes, A. Gold nanoparticle-based electrochemical biosensors. *Electrochim. Acta* **2008**, *53* (19), 5848−5866.
(11) Guschin, D. A.; Shkil, H.; Schuhmann, W. Electrodeposition polymers as immobilization matrices in amperometric biosensors: improved polymer synthesis and biosensor fabrication. *Anal. Bioanal. Chem.* **2009**, *395* (6), 1693−1706.
(12) Wang, J.; Jensen, U. B.; Jensen, G. V.; Shipovskov, S.; Balakrishnan, V. S.; Otzen, D.; Pedersen, J. S.; Besenbacher, F.; Sutherland, D. S. Soft Interactions at Nanoparticles Alter Protein Function and Conformation in a Size Dependent Manner. *Nano Lett.* **2011**, *11* (11), 4985−4991.
(13) Homola, J.; Yee, S. S.; Gauglitz, G. Surface plasmon resonance sensors: review. *Sens. Actuators, B* **1999**, *54* (1−2), 3−15.
(14) Elwing, H. Protein absorption and ellipsometry in biomaterial research. *Biomaterials* **1998**, *19* (4−5), 397−406.
(15) Kurrat, R.; Textor, M.; Ramsden, J. J.; Boni, P.; Spencer, N. D. Instrumental improvements in optical waveguide light mode spectroscopy for the study of biomolecule adsorption. *Rev. Sci. Instrum.* **1997**, *68* (5), 2172−2176.
(16) Seevers, R. H.; Counsell, R. E. Radioiodination techniques for small organic-molecules. *Chem. Rev.* **1982**, *82* (6), 575−590.
(17) Richter, R. P.; Brisson, A. Characterization of lipid bilayers and protein assemblies supported on rough surfaces by atomic force microscopy. *Langmuir* **2003**, *19* (5), 1632−1640.
(18) Malmstrom, J.; Agheli, H.; Kingshott, P.; Sutherland, D. S. Viscoelastic Modeling of highly hydrated laminin layers at homogeneous and nanostructured surfaces: Quantification of protein layer properties using QCM-D and SPR. *Langmuir* **2007**, *23* (19), 9760−9768.
(19) Rechendorff, K.; Hovgaard, M. B.; Foss, M.; Besenbacher, F. Influence of surface roughness on quartz crystal microbalance measurements in liquids. *J. Appl. Phys.* **2007**, *101* (11).
(20) Wilson, R.; Turner, A. P. F. Glucose oxidase: an ideal enzyme. *Biosens. Bioelectron.* **1992**, *7*, 165−185.
(21) Heller, A.; Feldman, B. Electrochemical glucose sensors and their applications in diabetes management. *Chem. Rev.* **2008**, *108* (7), 2482−2505.
(22) Wang, J. Electrochemical glucose biosensors. *Chem. Rev.* **2008**, *108* (2), 814−825.
(23) Shipovskov, S.; Trofimova, D.; Saprykin, E.; Christenson, A.; Ruzgas, T.; Levashov, A. V.; Ferapontova, E. E. Spraying enzymes in microemulsions of AOT in nonpolar organic solvents for fabrication of enzyme electrodes. *Anal. Chem.* **2005**, *77* (21), 7074−7079.
(24) Yang, S. M.; Jang, S. G.; Choi, D. G.; Kim, S.; Yu, H. K. Nanomachining by colloidal lithography. *Small* **2006**, *2* (4), 458−475.
(25) Robbie, K.; Brett, M. J. Sculptured thin films and glancing angle deposition: Growth mechanics and applications. *J. Vac. Sci. Technol., A* **1997**, *15* (3), 1460−1465.
(26) Robbie, K.; Beydaghyan, G.; Brown, T.; Dean, C.; Adams, J.; Buzea, C. Ultrahigh vacuum glancing angle deposition system for thin films with controlled three-dimensional nanoscale structure. *Rev. Sci. Instrum.* **2004**, *75* (4), 1089−1097.
(27) Attri, P.; Venkatesu, P.; Kumar, A. Activity and stability of [small alpha]-chymotrypsin in biocompatible ionic liquids: enzyme refolding by triethyl ammonium acetate. *Phys. Chem. Chem. Phys.* **2011**, *13* (7), 2788−2796.
(28) Roach, P.; Farrar, D.; Perry, C. C. Surface tailoring for controlled protein adsorption: Effect of topography at the nanometer scale and chemistry. *J. Am. Chem. Soc.* **2006**, *128* (12), 3939−3945.
(29) Jensen, U. B.; Lörcher, S.; Vagin, M.; Chevallier, J.; Shipovskov, S.; Koroleva, O.; Besenbacher, F.; Ferapontova, E. E. A 1.76 V hybrid Zn-O2 biofuel cell with a fungal laccase-carbon cloth biocathode. *Electrochim. Acta* **2012**, *62* (0), 218−226.
(30) Hoare, J. P. A Cyclic Voltammetric Study of the Gold-Oxygen System. *J. Electrochem. Soc.* **1984**, *131* (8), 1808−1815.
(31) Sauerbrey, G. Verwendung von Schwingquarzen zur Wägung dünner Schichten und zur Mikrowägung. *Z. Phys.* **1959**, *155* (2), 206−222.
(32) Kanazawa, K. K.; Gordon, J. G. Frequency of a quartz microbalance in contact with liquid. *Anal. Chem.* **1985**, *57* (8), 1770−1771.
(33) Voinova, M. V.; Rodahl, M.; Jonson, M.; Kasemo, B. Viscoelastic acoustic response of layered polymer films at fluid-solid interfaces: Continuum mechanics approach. *Phys. Scr.* **1999**, *59* (5), 391−396.
(34) Hook, F.; Voros, J.; Rodahl, M.; Kurrat, R.; Boni, P.; Ramsden, J. J.; Textor, M.; Spencer, N. D.; Tengvall, P.; Gold, J.; Kasemo, B. A comparative study of protein adsorption on titanium oxide surfaces using in situ ellipsometry, optical waveguide lightmode spectroscopy, and quartz crystal microbalance/dissipation. *Colloids Surf., B* **2002**, *24* (2), 155−170.
(35) Reimhult, E.; Larsson, C.; Kasemo, B.; Hook, F. Simultaneous surface plasmon resonance and quartz crystal microbalance with dissipation monitoring measurements of biomolecular adsorption events involving structural transformations and variations in coupled water. *Anal. Chem.* **2004**, *76* (24), 7211−7220.
(36) Liedberg, B.; Nylander, C.; Lundström, I. Surface plasmon resonance for gas detection and biosensing. *Sens. Actuators* **1983**, *4*, 299−304.
(37) Wong, C. M.; Wong, K. H.; Chen, X. D. Glucose oxidase: natural occurrence, function, properties and industrial applications. *Appl. Microbiol. Biotechnol.* **2008**, *78* (6), 927−938.
(38) Hecht, H. J.; Kalisz, H. M.; Hendle, J.; Schmid, R. D.; Schomburg, D. Crystal structure of glucose oxidase from aspergillus niger refined at 2.3 angstrom resolution. *J. Mol. Biol.* **1993**, *229* (1), 153−172.
(39) Szucs, A.; Hitchens, G. D.; Bockris, J. O. On the Adsorption of Glucose Oxidase at a Gold Electrode. *J. Electrochem. Soc.* **1989**, *136* (12), 3748−3755.
(40) Rechendorff, K.; Hovgaard, M. B.; Foss, M.; Zhdanov, V. P.; Besenbacher, F. Enhancement of protein adsorption induced by surface roughness. *Langmuir* **2006**, *22* (26), 10885−10888.
(41) Bartlett, P. N. *Bioelectrochemistry: Fundamentals, Experimental Techniques and Applications*; John Wiley & Sons: Hoboken, NJ, 2008.
(42) Kartashov, A. V.; Serafini, G.; Dong, M. D.; Shipovskov, S.; Gazaryan, I.; Besenbacher, F.; Ferapontova, E. E. Long-range electron transfer in recombinant peroxidases anisotropically orientated on gold electrodes. *Phys. Chem. Chem. Phys.* **2010**, *12* (34), 10098−10107.
(43) Bourdillon, C.; Demaille, C.; Moiroux, J.; Saveant, J. M. New insights into the enzymic catalysis of the oxidation of glucose by native and recombinant glucose oxidase mediated by electrochemically generated one-electron redox cosubstrates. *J. Am. Chem. Soc.* **1993**, *115* (1), 2−10.

(44) Du, J.; Yu, X.; Di, J. Comparison of the direct electrochemistry of glucose oxidase immobilized on the surface of Au, CdS and ZnS nanostructures. *Biosens. Bioelectron.* **2012**, *37* (1), 88−93.
(45) Bourdillon, C.; Demaille, C.; Moiroux, J.; Saveant, J. M. Analyzing product inhibition and pH gradients in immobilized enzyme films as illustrated experimentally by immunologically bound glucose oxidase electrode coatings. *J. Phys. Chem. B* **1999**, *103* (40), 8532−8537.
(46) Bao, J.; Furumoto, K.; Fukunaga, K.; Nakao, K. A kinetic study on air oxidation of glucose catalyzed by immobilized glucose oxidase for production of calcium gluconate. *Biochem. Eng. J.* **2001**, *8* (2), 91−102.